Scattering of low-energy (10 - 350 eV) light ions from Al(111); neutralization and dissociation

1997 J. Phys.: Condens. Matter 9 1919

(http://iopscience.iop.org/0953-8984/9/9/007)

J. Phys.: Condens. Matter **9** (1997) 1919–1930. Printed in the UK PII: S0953-8984(97)77723-3

Scattering of low-energy (10–350 eV) light ions from Al(111); neutralization and dissociation

Michio Okada†§ and Yoshitada Murata‡

† Department of Chemistry, Faculty of Science, Osaka University, 1-1 Machikaneyama-cho, Toyonaka, Osaka 560, Japan

‡ Division of Natural Sciences, The University of Electro-Communications, 1-5-1 Chofugaoka, Chofu, Tokyo 183, Japan

Received 10 September 1996, in final form 19 November 1996

Abstract. The incident-energy dependence and angular distribution of a scattered-D_2^+ yield were measured and compared with those of scattered-D^+ and scattered-He^+ yields. Below the incident energy of 80 eV, both resonance and Auger neutralization processes are considered to contribute to the ion-survival probability in D_2^+ and D^+ scattering, from the analysis based on the calculation by Imke *et al* (Imke U, Snowdon K J and Heiland W 1986 *Phys. Rev.* B **34** 41, 48). Above the incident energy of 80 eV, the electron promotion mechanism contributes additionally to the ion neutralization process, and causes the difference between He^+ and the other ions as regards the survival-ion yields. The threshold energy at which dissociated D^+ appears for D_2^+ incidence is ∼20 eV. The dissociated D^+ is considered to arise via reionization of a D atom which is dissociated from once-neutralized D_2 via impulsive collision.

1. Introduction

Low-energy ($\leqslant$100 eV) molecular ions are very interesting from the standpoint of exploring new pathways of chemical reaction on and with surfaces [1–4]. A physical view of the ion-survival probability in this low-energy region—below 100 eV—has been discussed on the basis of measuring the incident-energy dependence of the survival-ion yield [5]. In the case of rare-gas-ion scattering where Auger neutralization contributes mainly to the ion-survival probability, an empirical model in which the characteristic velocity varies with the depth to which the ion penetrates into the surface can explain well the dependence of the scattered-ion yield on the incident energy [6]. Furthermore, the rapid change in the survival-ion yield was discussed assuming two kinds of repulsive potential in the ion–surface interaction [7]. On the other hand, it is not clear whether the Auger neutralization process dominates the ion-survival probability in the low-energy reactive-ion scattering. Müller *et al* measured emitted-electron energy spectra from slow H^+ and H_2^+ ions (below 100 eV) colliding at grazing incidence with the W(110) surface, and reported that Auger capture involving two surface electrons is a dominant process for the electron emission from the clean surface [8]. Harder *et al* discussed the dissociation dynamics of fast-ionized-H_2^+ beams (surface-normal energies of 0.2–8 eV) meeting a Cu(111) surface at grazing incidence [9]. The results are interpreted in terms of charge transfer occurring to both the $b^3\Sigma_u^+$ and $X^1\Sigma_g^+$ states of H_2 with a branching ratio of the same order of magnitude, and using a potential energy surface

§ Author to whom any correspondence should be addressed.

0953-8984/97/091919+12$19.50

mediated by 'hot electrons' excited due to the fast H_2^+ particles. On the other hand, the findings by Schmidt *et al* for grazing incidence of low-energy H_2^+ ions have been interpreted in terms of the Auger and resonance capture processes and in terms of dissociation caused by dynamical screening [10].

In this paper, we try to elucidate which neutralization process (Auger and/or resonance neutralization) is dominant for determining the ion-survival probability in reactive-ion scattering, on the basis of the theoretical calculation performed by Imke *et al* [11]. Imke *et al* calculated the transition rate of the resonance neutralization in the H_2^+/Al system and discussed the molecular-orientation dependence of the transition rate. The calculation indicates that the determination of the dominant neutralization process may make it possible to discuss the molecular-orientation effect in the H_2^+ scattering.

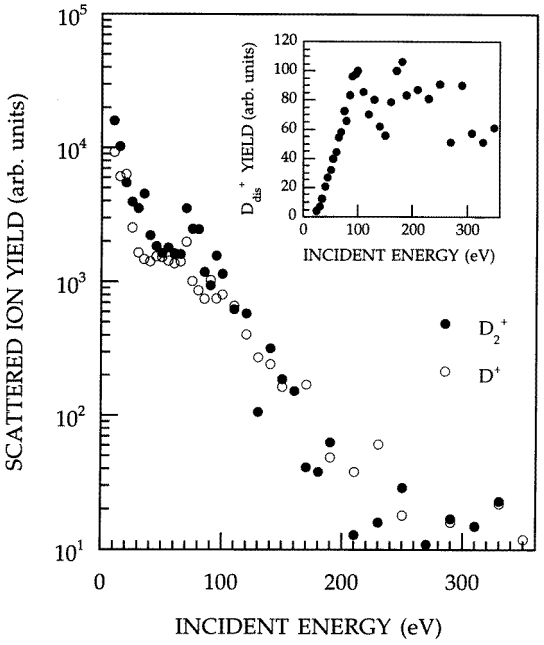

Figure 1. The incident-energy dependence of the scattered-D_2^+-ion (full circles) and scattered-D^+-ion (open circles) yields for 60° specular scattering along $\langle 11\bar{2} \rangle$ on Al(111) for D_2^+ and D^+ incidence, respectively. The inset shows the incident-energy dependence of the dissociated-D^+-ion yield for D_2^+ incidence. The yield is given in arbitrary units, in all of the figures in this paper.

During the interaction of a low-energy reactive ion, below 100 eV, with a metal surface, surface trapping is an important scattering process [12]. When an ion enters into the chemical-potential well and moves outward along the outgoing trajectory, a substantial amount of the surface-normal component of the kinetic energy will be dissipated via phonon and plasmon excitations and electron–hole-pair creation to the surface. Reactive ions will have a large cross section in inelastic scattering with substantial energy losses. When the normal energy of an ion is smaller than the potential barrier on the exit trajectory, the ion cannot escape and will be trapped in the direction parallel to the surface, which may induce skipping motion [13, 14]. Therefore, reactive ions are effectively neutralized during the surface trapping, because the surface residence time is elongated.

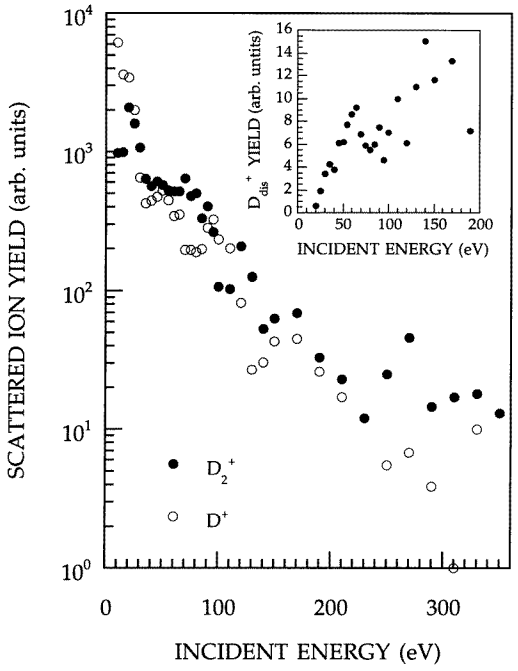

Figure 2. The incident-energy dependence of the scattered-D_2^+-ion (full circles) and scattered-D^+-ion (open circles) yields for 45° specular scattering along $\langle 11\bar{2} \rangle$ on Al(111) for D_2^+ and D^+ incidence, respectively. The inset shows the incident-energy dependence of the dissociated-D^+-ion yield for D_2^+ incidence.

Dissociative chemisorption and scattering are outcomes from the dissociation process. It is important to interpret the dissociation process from the microscopic point of view, e.g. via molecular-orientation effects [15]. Several models have been reported for the dissociation of scattered molecules. Gerber *et al* [16] proposed a rotational excitation model where a rotation torque works as a centrifugal force on the molecule, and constituent atoms are separated if the centrifugal force surmounts the dissociation barrier. The predominance of rotational excitation at low energy was also proposed by Kleyn and co-workers [17, 18]. At higher energies, they reported that the energy transfer to the vibrational modes during the collision is larger than that to the rotational modes [17]. Akazawa and Murata [12, 19] proposed a vibrational excitation mechanism for dissociation in the threshold energy region for dissociated-ion formation. The maximum in the angular distribution of the dissociated atoms appears in the supra-specular direction as a result of the impulsive dissociative collision [3, 12, 19]. On the other hand, several electronic mechanisms have also been proposed for dissociative scattering. Snowdon, Heiland, and co-workers [20, 21] proposed a model of dissociative electron attachment. When the excited state to which an electron is transferred is an anti-bonding or a predissociation state, the scattered molecule will be dissociated via neutralization. Gazuk and co-workers [22] proposed another electronic process for dissociation, which is referred to as dissociation via harpooning. The negative ion formed near the surface acts as a precursor to dissociation of the molecule [2, 23]. Recently, the dissociative scattering processes have been interpreted in the other ways: in terms of dynamical screening [10] and in terms of the potential energy surfaces via 'hot

electrons' [9].

In the D_2^+/Al(111) system, the electronic transition to the dissociative $b^3\Sigma_u^+$ state depends strongly on the molecular orientation [11]. So, the system is a good candidate for use in the study of the molecular-orientation effect on neutralization and dissociative scattering.

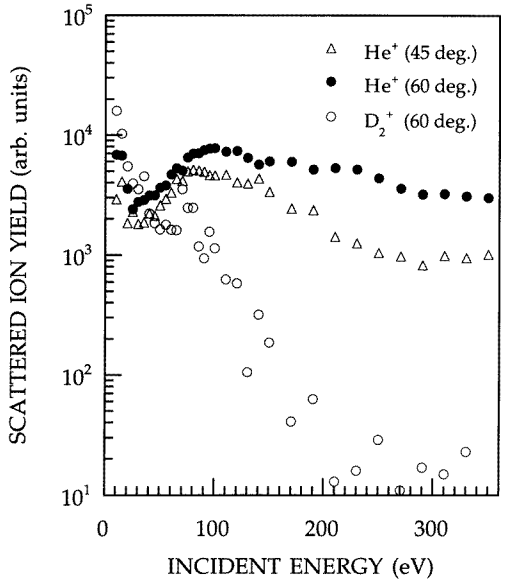

Figure 3. The incident-energy dependence of the scattered-He^+-ion (full circles) and scattered-D_2^+-ion (open circles) yields for 60° specular scattering and the scattered-He^+-ion yield (open triangles) for 45° specular scattering along $\langle 11\bar{2}\rangle$ on Al(111).

2. Experimental details

The ion source is a Menzinger-type plasma source, where the anode voltage was set within the range 50–150 V, and 100–200 mA arc current was obtained. The beam current fluctuation on the target was kept within 5% for a few hours. Ions are extracted, accelerated and mass selected. Neutral species are excluded by bending the ion trajectory with an electromagnet of the mass selector installed in an ultrahigh-vacuum chamber. Finally, the ions are successively decelerated by passing them through a deceleration lens system. The incident-ion current was 1–20 nA even at low energies below 100 eV.

Only scattered positive ions were detected with a quadrupole mass filter which is rotatable around the crystal surface. The trajectories of ions after passing through the mass filter were bent by 90° with a deflecting plate mounted in front of an electron multiplier in order to remove neutral species. The voltage applied to the deflecting plate was adjusted for the maximum intensity of detected ions. The ion yield was obtained by integrating the mass peak and normalized with the incidence-beam current. The angles of incidence are 60° and 45° from the surface normal. The scattering plane includes the $\langle 11\bar{2}\rangle$ azimuth.

An Al single crystal oriented by x-ray diffraction was cut parallel to the (111) lattice plane. The Al(111) surface was mechanically polished down to 0.06 μm and was cleaned

by repeated Ar^+-ion bombardment and annealing at 470–670 K. Low-energy electron diffraction showed a sharp (1×1) pattern and the Auger electron spectrum showed no detectable contamination. The surface cleanliness was also verified by secondary-ion-emission measurements.

3. Results

3.1. The incident-energy dependence of the scattered-ion yield

Figures 1 and 2 show the incident-energy dependence of the scattered-ion yield in the specular scattering for 60° and 45° incidences, respectively. The survival-ion yields for the D_2^+ and the D^+ incidence are of the same order of magnitude for any incident energies below 350 eV. The survival-ion yields decrease monotonically with incident energy for both D_2^+ and D^+ for incident energies above 100 eV. We can compare the survival-ion yields for D_2^+ with those for He^+ shown in figure 3. The V-shaped energy dependence of the survival-ion yield for He^+ scattering was interpreted using a simple empirical model using the modified Hagstrum formula [5, 6]. At incident energies above 100 eV, the energy dependence of the D_2^+ yield is quite different from that of the He^+ yield. The scattered-ion yield of He^+ is 1–2 orders of magnitude larger than that of D_2^+ and D^+.

The insets in figures 1 and 2 show the incident-energy dependence of the dissociated-D^+ yield for the D_2^+ incidence. The dissociated-D^+ yield increases with increasing incident energy of D_2^+ from the threshold energy at which dissociated D^+ appears. The threshold energy for dissociated D^+ is ∼20 eV and is independent of the incidence angle.

3.2. The polar-angle distribution of the scattered-ion yield

Figures 4 and 5 show the polar-angle distributions of the scattered-D_2^+ and scattered-D^+ yields in the scattering plane along the $\langle 11\bar{2} \rangle$ azimuth, respectively. The angular distribution of D_2^+ is similar to that of D^+, when compared in the same scattering geometry. The maximum position in the lobe of scattered D_2^+ and D^+ is located at ∼10° from the surface parallel. The polar-angle distribution of the scattered ions is narrow for the 60° incidence, while the lobe width for the 45° incidence is broader. Moreover, double peaks are clearly observed for the 45° incidence for both D_2^+ and D^+ with an incident energy of 50 eV. It should be noted that the maximum position in the angular distribution of scattered He^+ is located approximately in the specular direction [24].

The polar-angle distribution of the dissociated-D^+ yield for the D_2^+ incidence is also shown in figure 4. The lobe of the dissociated-D^+ yield is broad as compared to those of scattered D_2^+ and D^+ for both 60° and 45° incidences and is located at the supra-position.

4. Discussion

4.1. The neutralization process at incident energies below 80 eV; an empirical model based on the calculation by Imke et al [11]

Figure 6 shows an energy diagram of free D_2, D, and He atoms, which is relevant to the discussion of the charge exchange of D_2^+, D^+, and He^+ with the Al(111) surface [25, 26]. The work function of Al(111) used here is 4.24 eV [27]. For D_2^+, resonant electron transfers from the occupied valence states of the metal to the $b^3\Sigma_u^+$ and $X^1\Sigma_g^+$ states of D_2 are energetically allowed over a wide range of internuclear separation. Auger

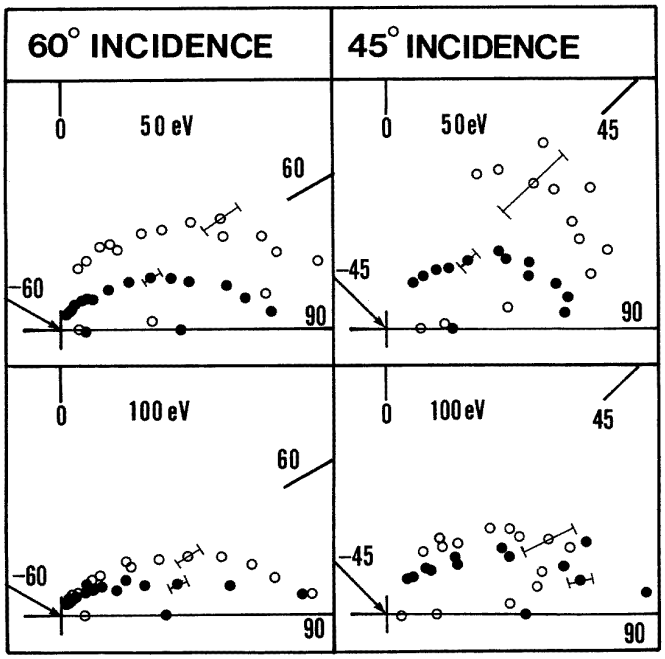

Figure 4. The polar-angle distributions of the scattered-D_2^+-ion (full circles) and the scattered-D_{dis}^+-ion (open circles) yields for D_2^+ incidence with incident energies of 50 and 100 eV. The angles of incidence from the surface normal are 60° and 45° for the left-hand and the right-hand parts of the figure, respectively. The scale of the D_2^+-ion yield is different from that of the D_{dis}^+-ion yield.

electron transition from the occupied valence states to the $X^1\Sigma_g^+$ state is also energetically allowable. Both resonant and Auger electron transitions to $^2S_{1/2}$ ($n = 1$) are allowed for D^+. Auger electron capture to $^1S_0$ and the Auger de-excitation process following the resonant neutralization to $^3S_1$ are possible for He^+. The latter process for He^+ may give a small contribution to the charge-exchange process, because the image-potential effect shifts up the energy level of $^3S_1$ by 1–2 eV.

We construct a simple model with the following assumptions. (a) The overlap of the spatial part of the $X^1\Sigma_g^+$ state of D_2 with the valence state of Al is nearly equal to that of the 1s state of D with the valence state of Al, when compared at the same distance from the Al surface. (b) D_2^+ and D^+ are scattered by the same potential wall. The latter assumption is considered to be reasonable because the angular distributions of the scattered D_2^+ and D^+ ions are similar, as shown in figures 4 and 5. For D_2^+, the dissociation via rotational and/or vibrational excitation may contribute to the survival probability of D_2^+ and may decrease the survival-ion yield by a factor of magnitude. In the present study, we discuss only the difference in the order of magnitude for the survival-ion yield. Moreover, the incident-energy dependence of the survival-D_2^+ yield is similar to that of D^+ at any incident energy below 350 eV, as seen in figures 1 and 2. This result may indicate that the mechanical dissociation gives a minor contribution to the survival-ion yield of D_2^+ in the present case. The mechanical dissociation is considered to become important for discussing the yields of the scattered neutral D_2 and dissociated particles of D and D^+. So, we discuss in this section only Auger and resonance neutralizations for the ion-survival probability. The

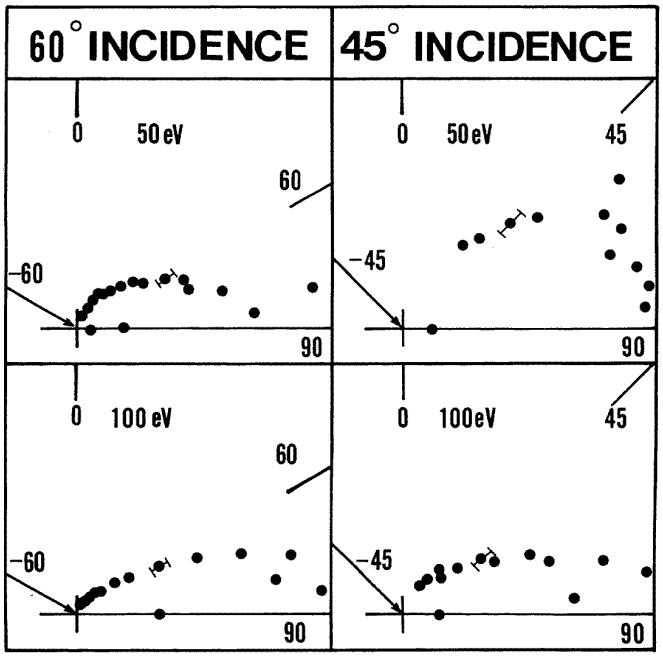

Figure 5. The polar-angle distributions of the scattered-D^+-ion yield for D^+ incidence with incident energies of 50 and 100 eV. The angles of incidence from the surface normal are 60° and 45° for the left-hand and the right-hand parts of the figure, respectively.

discussion described here does not include neutralization via electron promotion, because the neutralization via electron promotion which causes the difference between the ion yield of He^+ and those of reactive ions (D_2^+ and D^+) is dominant at incident energies above 80 eV, as seen in figures 1 and 2. The neutralization via electron promotion will be discussed below in section 4.2.

The transition rate of resonance neutralization to the $b^3\Sigma_u^+$ and $X^1\Sigma_g^+$ states can be described as $A\exp(-as)$ and $B\exp(-bs)$ [11], where A, B, a, and b are constant values and s is the distance between the surface and a projectile. The transition rate of Auger neutralization to $X^1\Sigma_g^+$ can be assumed to be nearly equal to that of resonance neutralization to $X^1\Sigma_g^+$. According to the calculation performed by Snowdon *et al*, the resonance and the rate of Auger transition to the 1s state of H on a jellium (Al) surface are of comparable magnitude when both mechanisms are energetically allowed [28]. So, we can describe the transition rate of Auger neutralization to $X^1\Sigma_g^+$ as $B\exp(-bs)$. As a result, the transition rate of the neutralization of D_2^+ ions is described as

$$R_a(s) = A\exp(-as) + 2B\exp(-bs). \tag{1}$$

Next, we will discuss the transition rates of resonance and Auger neutralization to the 1s state of D. In the case of D_2^+ scattering, the spin wavefunction of the final D_2 state should be taken into consideration. A two-electron state in D_2 is formed from two one-electron states through the electron transfer from the metal surface to the D_2^+. The total wavefunction describing the final molecular D_2 state must be anti-symmetric. The spin wavefunction of the final molecular state must be anti-symmetric after the electron transfer to $X^1\Sigma_g^+$ of D_2. So, the allowed number of the spin wavefunctions of $X^1\Sigma_g^+$ is one quarter

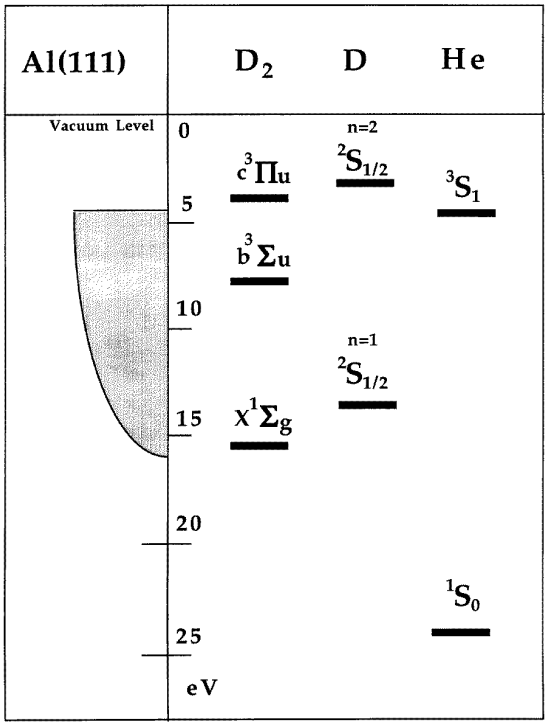

Figure 6. The energy diagram relevant to the neutralization interpretation of D_2^+, D^+, and He^+ ions on an Al(111) surface.

of the total number of spin wavefunctions. On the other hand, it is not necessary to take the spin wavefunction in D^+ scattering into consideration. Therefore, the transition rate of the neutralization to the 1s state of D is four times as large as that to the $X^1\Sigma_g^+$ state of D_2. So, the transition rate of resonance and Auger neutralization can be described as

$$R_b(s) = 8B\exp(-bs). \tag{2}$$

The attractive part of the ion–surface interaction potential is considered to play an important role in the reactive-ion scattering. In the present discussion, however, the ion penetration depth is calculated with the repulsive potential wall of $C\exp(-cs)$ where C and c are constant values, because the depth of penetration of an ion into the classical potential is mainly determined by the repulsive part of the interaction potential. The constants a, b, and c are determined from the overlap of the related wavefunctions. Therefore, $a \approx b$ and $b \approx c$ are considered to be good approximations without any consideration of the molecular orientation, because all three constants represent the overlap of the wavefunctions of the Σ state and the metal. The ion-survival probability is given by

$$P = \exp\{-v_c[(1/v_{\text{in}}) + (1/v_{\text{out}})]\} \tag{3}$$

where v_c is a characteristic velocity and v_{in} and v_{out} are the surface-normal components of the velocities in the incoming and the outgoing trajectory, respectively [29]. The closest approach distance s_0 in the specular scattering is given by $s_0 = (-1/c)\ln(E_n/C)$, where E_n is the surface-normal component of the kinetic energy. So, from equation (1), the

characteristic velocity in the D_2^+ scattering is given [6, 7] by

$$v_{ca} = (A/a + 2B/b)E_n/C. \tag{4}$$

From equation (2), the characteristic velocity in D^+ scattering is given by

$$v_{cb} = 8BE_n/\sqrt{2}bC \tag{5}$$

where the factor of $1/\sqrt{2}$ is due to the difference between the velocities of D^+ and D_2^+ at the same energy and is included in the characteristic velocity. According to the calculation by Imke *et al*, $A \approx 5.5B$ and $a \approx 0.82b$ [11]. With the approximation $b \approx c$, the relation $v_{ca} \approx 1.5v_{cb}$ is obtained from equations (4) and (5). Akazawa and Murata reported that the ion-survival probability is mainly determined by Auger neutralization to the ground state of the particles [5]. If only Auger neutralization contributes to the ion-survival probability, the relation $v_{cb} \approx 2.8v_{ca}$ is obtained. Thus, the survival-D^+ yield is expected to be much smaller than the D_2^+ yield from equation (3), and this result is inconsistent with the experimental data. On the other hand, the relation $v_{ca} = 1.5v_{cb}$, deduced on the assumption that both Auger and resonance neutralization contribute, is consistent with the experimental result that the D_2^+ and D^+ yields are of almost the same order of magnitude. Therefore, in the present case, both Auger and resonance neutralization processes are considered to contribute to the ion-survival probability. The probability of the Auger neutralization for D^+ is expected to be larger than that for D_2^+ according to the above-mentioned discussion. Müller *et al* reported that the electron emission coefficients for H_2^+ collisions with clean metals are lower than those for H^+ collisions [8]. This result supports that expected difference between the Auger neutralization probabilities of D_2^+ and D^+.

For D_2^+, resonance neutralization to $b^3\Sigma_u^+$ contributes substantially to the ion-survival probability. Imke *et al* reported that the rate of transition to the $b^3\Sigma_u^+$ state has a strong angular dependence. The rotational motion is frozen within the collision time $\sim 10^{-15}$ s, and, as a result, molecular orientation to the surface is kept in the interaction region until the molecule reaches the classical turning point along the trajectory. A large proportion of the surviving D_2^+ ions are considered to take the molecular orientation parallel to the surface at the classical turning point of the scattering trajectory [11]. The D^+ yield is expected to be larger than the D_2^+ yield according to the relation $v_{ca} = 1.5v_{cb}$. However, the D^+ yield is smaller than the D_2^+ yield in the present experiments, as seen in figures 1 and 2. This result might be due to the difference in the scattering cross section and/or due to the molecular-orientation effect on neutralization where the transition rate is small for the molecule with its axis parallel to the surface [11].

4.2. The neutralization process at incident energies above 80 eV

Next, we discuss the survival-ion yield in the higher-incident-energy region. The model for the incident-energy dependence of the neutralization probability proposed by Akazawa and Murata [6] can be extended to the neutralization process including resonance neutralization. For $s_0 \geqslant s_c$, the characteristic velocity v_c is given by equations (4) and (5), and for $s_0 \leqslant s_c$, v_c takes a constant value, where s_0 is the distance between the surface and the classical turning point of the trajectory, and s_c is a critical closest approach distance. As a result, a V-shaped energy dependence of the ion yield is expected in the present case. However, a V-shaped dependence is not clearly observed in D^+ and D_2^+ scattering. On the other hand, a V-shaped energy dependence is clearly observed in the He^+ scattering shown in figure 3. The scattered-ion yield for He^+ incidence with energies above 100 eV is 1–2 orders of magnitude larger than that for D^+ and D_2^+ incidence. These results are considered to be due

to collisional neutralization via electron promotion. The ionization potential for He is much larger than that of D and D_2, as shown in figure 6. So, electron promotion occurs more effectively for D^+ and D_2^+ than for He^+, when compared at the same kinetic energy, and, as a result, neutralization via electron promotion for D^+ and D_2^+ starts at a lower incident energy compared to that for He^+. It should be noted that H_2^+ ions were observed in the collision of a H_2 molecule with a Ag(111) target at incident energies above 70 eV [18]. On the other hand, the reionization of He on an Al surface was not observed below the incident energy of 300 eV [30]. Enhanced neutralization probability via electron promotion smears out the V-shaped energy dependence for reactive ions (D^+ and D_2^+). There are two types of neutralization process via electron promotion. One is an atomic-like process where two atomic levels cross adiabatically in the quasimolecular state at the impact collision and then neutralization occurs [31, 32]. The other is an enhanced-resonance process via electron promotion [33]. The survival-ion yields of D_2^+ and D^+ are nearly equal at the incident energies above 100 eV shown in figures 1 and 2. In the collisional neutralization, the Al–D quasimolecular state is produced, and neutralization via level crossing between the 3p level of Al and the 1s level of D will occur for both D_2^+ and D^+. As a result, nearly the same neutralization cross section can be expected. It is also possible that the 1s level of D and $X^1\Sigma_g^+$ of D_2, which have the nearly the same energy level, as shown in figure 6, will promote and interact strongly with the valence electrons of Al. The molecular-orientation effect is considered to be small in the neutralization via electron promotion.

4.3. The polar-angle distribution of the scattered D_2^+ and D^+ ions

The angular distribution of the scattered ions for D_2^+ and D^+ incidence is shown in figures 4 and 5, respectively. For the 60° incidence, the maximum lobe position of scattered D_2^+ ions is located at ∼10° from the surface parallel, and the distributions of the scattered ions are narrow. The lobe shape and position suggest that the scattered ions in this direction were once trapped into the chemical interaction potential. As mentioned above, a surviving D_2^+ may have its molecular axis nearly parallel to the surface at the turning point of the scattering trajectory. The chemical interaction is considered to be strong for this molecular orientation. The lobe width for the D_2^+ scattering observed at 50 eV is slightly broader than that at 100 eV. This tendency is more clearly observed for the 45° incidence. The ions scattered into a small angle through impact collisions will be effectively neutralized via collisional neutralization above 80 eV, as discussed in section 4.2. Electron promotion occurs effectively with small impact parameters between projectiles and surface atoms, because the kinetic energy of the projectile is effectively changed into electronic energy in a collision with a small impact parameter.

For the D_2^+ and D^+ incidence with an incident energy of 50 eV, the angular distribution for 45° incidence is very different from that for 60° incidence. The scattering lobe for 45° incidence is broader than that for 60° incidence, and shows double peaks in the angular distribution, as seen in figures 4 and 5. This can be explained as a surface rainbow [6]. For 45° incidence, a particle is scattered from a more corrugated potential wall than in the case of the 60° incidence. So the rainbow effect can be clearly observed for 45° incidence. The peak corresponding to the smaller angle from the surface normal is considered to originate from a single-collision scattering with a small impact parameter. The D_2^+ and D^+ scattered with such a small impact parameter will be effectively neutralized via electron promotion for higher incident energy, which smears out the surface rainbow effect at the incident energy of 100 eV shown in figures 4 and 5.

4.4. Dissociative scattering of D_2^+

The lobe of the dissociated D^+ is broad and is located at the supra-position of the lobes of the scattered D_2^+ and D^+, as shown in figures 4 and 5. So, the dissociation via translational-to-internal energy transfer through an impulsive collision is considered to be a dominant dissociation process near the threshold energy of dissociation, which is proposed by Akazawa and Murata (the vibrational excitation mechanism) [12, 19] and Kleyn and co-workers (the rotational excitation mechanism) [17, 18]. In the present case, the mechanical dissociation is considered to give a small contribution to the D_2^+-survival probability, as discussed in section 4.1.

The threshold energy for detecting dissociated D^+ is $\sim$20 eV which is independent of the incidence angle, as shown in the insets of figures 1 and 2. The estimation of the threshold energy for dissociation can be carried out on the basis of the vibrational excitation model proposed by Akazawa and Murata [12, 19]. According to this model, the collinear collision between a molecule and a target atom is effective for dissociation. The threshold energy is calculated by a simple equation, assuming collision of an AB molecule from an atom B onto a surface atom C collinearly keeping the molecular axis aligned with the moving direction. It is also assumed that an AB^+ molecule is harmonic or a Morse oscillator, initially at rest, and that the interaction between atoms B and C is purely repulsive, as expressed by the Born–Mayer potential. A reasonable analytical approximation for the energy transfer is known [34]. In the case of a D_2^+ collision with Al, the calculated threshold energy is $\sim$4 eV, which is much smaller than the total and normal energy of the observed threshold. This trend is also observed in the molecular-ion scattering by Pt(001) [12, 19]. It may be difficult to consider the reionization process of once-dissociated D in this energy region on the basis of the energy diagram shown in figure 6. However, since the velocity of the particle is large and the interaction potential is of short range, a non-adiabatic process via electron promotion is considered to be possible even in the observed threshold energy region of $\sim$20 eV in the collision with a very small impact parameter. This type of non-adiabatic charge-exchange process becomes dominant above the incident energy of 80 eV, as discussed in section 4.2.

The dissociated D^+ is considered to originate in the reionization of the D atom which is dissociated from once-neutralized D_2 via impulsive collision, and the observed threshold energy $\sim$20 eV corresponds to the reionization threshold. It should be noted that the charge transfer between a projectile and the Al surface appears during the sputtering at the incident energy of $\sim$35 eV for D_2^+, D^+, and He^+ [35].

5. Summary

Both resonance and Auger neutralizations are considered to contribute to the ion-survival probability in the low-energy D_2^+ and D^+ scattering, at incident energies below 80 eV, as concluded from the simple model based on the calculation by Imke *et al* [11]. The molecular axis of the surviving D_2^+ is supposed to be dominantly parallel to the surface at the turning point along the scattering trajectory from the calculation by Imke *et al* [11]. For incident energies above 80 eV, the neutralization process via electron promotion becomes dominant for D_2^+ and D^+ and causes the difference between the ion yield of He^+ and those of the reactive ions (D_2^+ and D^+). The dissociation of D_2^+ may occur via translational-to-internal energy transfer in the impulsive collision from the angular distribution of the dissociated D^+. The threshold energy $\sim$20 eV at which the dissociated D^+ is detected is considered to be the incident energy at which reionization of the dissociated D starts through impulsive collisions.

Acknowledgment

We are very grateful to Dr Rob Lahaye for valuable discussions.

References

[1] Kasi S R, Kang H, Sass C S and Rabaleis J W 1989 *Surf. Sci. Rep.* **10** 1
[2] Haochang P, Horn T C M and Kleyn A W 1986 *Phys. Rev. Lett.* **57** 3035
[3] Reijnen P H F, van Slooten U and Kleyn A W 1991 *J. Chem. Phys.* **94** 695
[4] Akazawa H and Murata Y 1988 *J. Chem. Phys.* **88** 3317
[5] Akazawa H and Murata Y 1988 *Phys. Rev. Lett.* **61** 1218
[6] Akazawa H and Murata Y 1989 *Phys. Rev.* B **39** 3449
[7] Murata Y, Fukutani K and Nakatsuji H 1996 *Surf. Sci.* **363** 112
[8] Müller H, Hausmann R, Brenten H and Kemper H 1993 *Surf. Sci.* **284** 129
[9] Harder R, Nesbitt A, Herrmann G, Tellioglu K, Rechtien J H and Snowdon K J 1994 *Surf. Sci.* **316** 63
[10] Schmidt K, Franke H, Schlathölter T, Höfner C, Närmann A and Heiland W 1994 *Surf. Sci.* **301** 326
[11] Imke U, Snowdon K J and Heiland W 1986 *Phys. Rev.* B **34** 41
Imke U, Snowdon K J and Heiland W 1986 *Phys. Rev.* B **34** 48
[12] Akazawa H and Murata Y 1990 *J. Chem. Phys.* **92** 5551
Akazawa H and Murata Y 1990 *J. Chem. Phys.* **92** 5560
[13] Snowdon K J, O'Connor D J and MacDonald R J 1988 *Phys. Rev. Lett.* **61** 1760
Snowdon K J, O'Connor D J and MacDonald R J 1989 *Surf. Sci.* **221** 465
[14] Rechtien J H, Mix W and Snowdon K J 1991 *Surf. Sci.* **248** 27
Mix W, Rechtien, J H, Danailov D and Snowdon K J 1991 *Nucl. Instrum. Methods* B **58** 365
[15] Rechtien J H, Mix W and Snowdon K J 1991 *Surf. Sci.* **259** 26
[16] Gerber R B and Elber R 1983 *Chem. Phys. Lett.* **102** 466
Gerber R B and Amirav A 1986 *J. Chem. Phys.* **90** 4483
[17] van den Hoek P J and Kleyn A W 1986 *J. Chem. Phys.* **90** 4483
[18] van Slooten U, Andersson D, Kleyn A W and Gislason E A 1991 *Chem. Phys. Lett.* **185** 440
[19] Akazawa H and Murata Y 1989 *Surf. Sci.* **207** L971
[20] Willerding B, Heiland W and Snowdon K J 1984 *Phys. Rev. Lett.* **53** 2031
[21] Imke U, Schubert S, Snowdon K J and Heiland W 1987 *Surf. Sci.* **189+190** 960
[22] Gazuk J W and Holloway S 1986 *J. Chem. Phys.* **84** 3502
Gazuk J W 1987 *J. Chem. Phys.* **86** 5169
[23] Reijnen P H F, van den Hoek P J, Kleyn A W, Imke U and Snowdon K J 1989 *Surf. Sci.* **221** 427
[24] Okada M and Murata Y 1993 *Surf. Sci.* **283** 41
[25] Moore C E 1949, 1952, 1958 *Atomic Energy Levels* NBS Circular No 467, vols 1–3 (Washington, DC: US Government Printing Office)
[26] Huber K P and Herzberg G 1979 *Constants of Diatomic Molecules (Molecular Spectra and Molecular Structure 4)* (New York: Van Nostrand-Reinhold)
[27] Grepstad J K, Gartland P O and Slagsvold B J 1976 *Surf. Sci.* **57** 348
[28] Snowdon K J, Hentschke R, Narmann A and Heiland W 1986 *Surf. Sci.* **173** 581
[29] Hagstrum H D 1977 *Inelastic Ion–Surface Collisions* ed N H Tolk, J C Tully, W Heiland and C W White (New York: Plenum) p 1
[30] Aono M and Souda R 1987 *Nucl. Instrum. Methods* B **27** 55
[31] Boers A L 1984 *Nucl. Instrum. Methods* B **4** 98
Verhey L K, Poelsema B and Boers A L 1976 *Nucl. Instrum. Methods* **132** 565
[32] Lichten W 1980 *J. Phys. Chem.* **84** 2102
Barat M and Lichten W 1972 *Phys. Rev.* A **6** 211
[33] Souda R, Yamamoto K, Tilley B, Hayami W, Aizawa T and Ishizawa Y 1994 *Phys. Rev.* B **50** 18 489
[34] Rapp D and Kassel T 1969 *Chem. Rev.* **69** 61
[35] Okada M and Murata Y 1994 *Surf. Sci.* **311** 254